

A NOVEL QUAD-MODE RESONATOR AND ITS APPLICATION TO DUAL-BAND BANDPASS FILTERS

**Shou-Jia Sun^{*}, Lei Lin, Bian Wu, Kun Deng,
and Chang-Hong Liang**

National Key Laboratory of Antennas and Microwave Technology,
Xidian University, Xi'an 710071, P. R. China

Abstract—In this paper, a novel square-loop quad-mode resonator is presented. Due to its symmetry, the even-odd-mode method is utilized to analyze the resonant characteristics. Two modes resonating at lower frequencies are employed to construct the first passband, and other two form the second passband. Meanwhile, both passband center frequencies can be controlled by the corresponding physical dimensions. Two dual-band bandpass filters (BPFs) without and with source-load coupling operating at 2.4 and 3.5 GHz are designed based on the proposed quad-mode resonator. Due to the source-load coupling, the passband selectivity and band-to-band isolation of the latter one are better than those of the former one. For demonstration, these two filters are fabricated and measured, and the measured results show good agreement with the simulated ones.

1. INTRODUCTION

Dual-band BPFs [1–3] have played an important role in recent multi-band wireless systems. Therefore, it is highly desirable to develop various dual-band BPFs, and many reports about various dual-band BPFs have been presented. Stepped-impedance resonators (SIRs) and stub-loaded resonators (SLRs) are good candidates in dual-band BPFs design [4–7]. In this way, there are at least two resonators required. For a compact size, filters based on dual-mode resonators have been attracting much more attention [8–12]. In [13–19], a single dual-mode resonator is employed to realize a dual-band bandpass filter (BPF) with compact size and high passband selectivity. Here,

Received 16 September 2013, Accepted 10 October 2013, Scheduled 10 October 2013

* Corresponding author: Shou-Jia Sun (sunshoujia@gmail.com).

the first-order harmonic is adopted to form the second passband. Recently, quad-mode resonators have been utilized to design dual-band BPFs by splitting their four resonant modes [20, 21]. Among them, a transmission zero used to separate the four resonant modes is introduced by the folded stubs. So far, the reports in this aspect are few, and there is still much research work to do.

This paper presents a novel square-loop quad-mode resonator, and the even-odd-mode method is utilized to analyze its resonant characteristics. The first two resonant modes with lower frequencies are employed to construct the first passband, and the other two modes with higher frequencies form the second passband. During this analysis, both passband center frequencies can be freely chosen by tuning the corresponding physical dimensions. Two dual-band BPFs without and with source-load coupling are designed based on the proposed quad-mode resonator. Both of them work at 2.4 GHz for WLAN and 3.5 GHz for WiMax, and the latter one with source-load coupling exhibits good passband selectivity and band-to-band isolation. For demonstration, both of them were fabricated and measured, and the measured results show good agreement with the simulated ones.

2. ANALYSIS OF THE PROPOSED QUAD-MODE RESONATOR

Figure 1(a) shows the geometrical schematic of the proposed square-loop quad-mode resonator. There are four points P_i ($i = 1, \dots, 4$) along the square loop: point P_1 is short circuited, a short-stub with electrical length θ_1 and admittance Y_1 is loaded at point P_3 , and a pair of identical short-stubs with electrical length θ_2 and admittance Y_2 are loaded at points P_2 and P_4 , respectively.

Because the proposed quad-mode resonator is symmetrical along the plane P_1 - P_3 , the even-odd-mode analysis is adopted to investigate its resonant characteristics. Its even- and odd-mode equivalent circuits are shown in Figure 1(b) and Figure 1(c), respectively. The short-stub with electrical length θ_1 is bisected under the even-mode excitation, and its width in Figure 1(b) is half what it was. In addition, it can be observed from Figure 1(c) that this circuit is still symmetrical, and then the even-odd-mode analysis is applied once again to calculate its resonant characteristics. The even- and odd-mode equivalent circuits of Figure 1(c) are illustrated in Figure 1(d) and Figure 1(e), respectively. Here, the width of the short-stub with electrical length θ_2 in Figure 1(d) is half what it was. On the basis of a transmission line theorem under the condition $Y = Y_1 = Y_2$, the resonant conditions for these equivalent

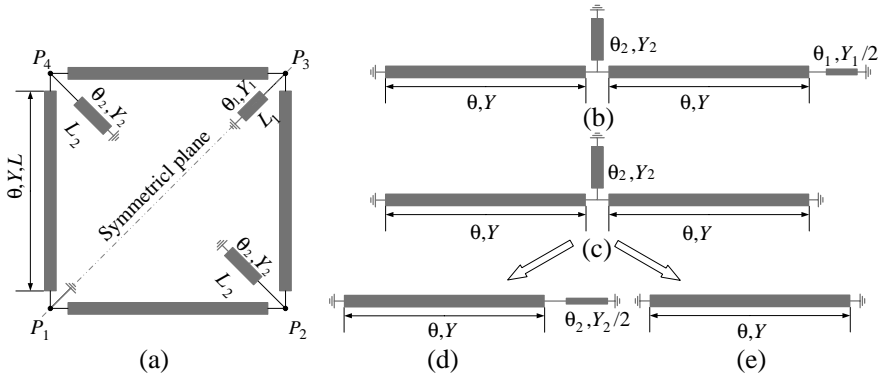


Figure 1. (a) Schematic of the proposed dual-band BPF. (b) Even- and (c) odd-mode equivalent circuits. (d) Even- and (e) odd-mode equivalent circuits of (c).

circuits can be given as follows

$$(1 - 2 \tan \theta_1 \cdot \tan \theta_2) \cdot \tan^2 \theta + 2(\tan \theta_1 + \tan \theta_2) \cdot \tan \theta + 2 \tan \theta_1 \cdot \tan \theta_2 = 0 \quad \text{for Figure 1(b)} \quad (1)$$

$$\tan \theta + 2 \tan \theta_2 = 0 \quad \text{for Figure 1(d)} \quad (2)$$

$$\theta = \frac{\pi}{2} \quad \text{for Figure 1(e)} \quad (3)$$

Obviously, four modes can be derived from the above equations. Two resonant frequencies can be obtained from (1), and another two resonant frequencies can be deduced from (2) and (3), respectively. Meanwhile, once the perimeter of the square loop resonator is fixed, the one resonant frequency derived from (3) remains constant. Here, two variables a_1 and a_2 are defined as:

$$a_1 = \frac{\theta_1}{\theta} \quad \text{and} \quad a_2 = \frac{\theta_2}{\theta} \quad (4)$$

According to the above resonant conditions, Figure 2 shows the variations of the resonant frequencies against a_1 and a_2 . Among them, f_1 and f_3 are derived from (1), and f_2 and f_4 are calculated from (2) and (3) respectively. It can be firstly observed that these four modes can form two passbands: f_1 and f_2 construct the first one, f_3 and f_4 form the second one. The variation of a_1 only changes f_1 and f_3 , and therefore, the length L_1 of the short-stub loaded at P_3 will control both passband in-band coupling strengths simultaneously. Lastly, the variation of a_2 has much more influence on the first passband than the

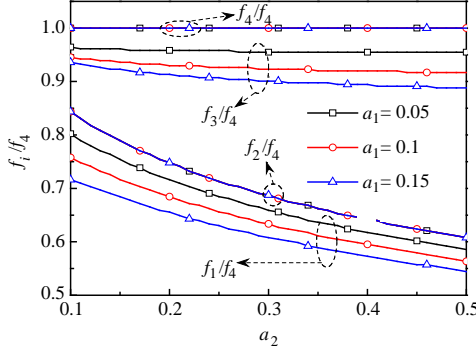


Figure 2. The variations of frequencies ratios against a_1 and a_2 .

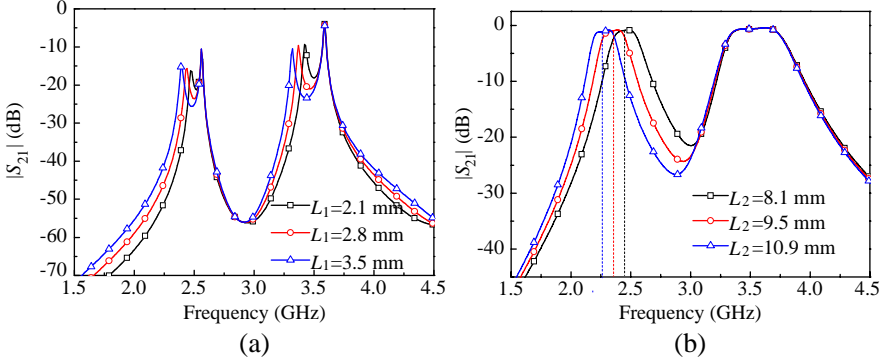


Figure 3. The transmission responses under different length (a) L_1 and (b) L_2 .

second passband, and therefore, the length L_2 of the short-stubs loaded at points P_2 and P_4 can be used to change the first passband center frequency, while there is almost no influence on the second passband, i.e., both passband center frequencies can be controlled by the lengths L and L_2 .

The variations of transmission responses under different lengths L_1 and L_2 are illustrated in Figure 3(a) and Figure 3(b), respectively. It can be observed from Figure 3(a) that the variation of L_1 affects f_1 and f_3 , while f_2 and f_4 remain constant. In addition, as can be seen from Figure 3(b), the variation of length L_2 changes the first passband center frequency, and the second passband is almost unchanged. These conclusions are in accordance with the above analysis.

3. FILTER DESIGN FABRICATION AND MEASUREMENT

Based on the above analysis, in this section two dual-band BPFs without and with source-load coupling based on the proposed quad-mode resonator are designed, fabricated and measured.

3.1. Dual-band BPF I without Source-load Coupling

The configuration of a dual-band BPF I operating at 2.4 and 3.5 GHz is shown in Figure 4, and all the short-circuit points are realized by ground via-holes with a diameter of 1 mm. Firstly, the length L or the perimeter of the square-loop is tuned to meet the second passband center frequency. Secondly, the first passband center frequency can be achieved by changing the length L_2 , meanwhile, minor adjustment about the length L can be made to guarantee the second passband remains the same. Thirdly, the fractional bandwidth (FBW) of the first passband with return loss 20 dB is 4.2%, and its in-band coupling coefficient $m_{1,2} = 0.069$ can be obtained according to filter synthesis in [22]. Based on the above analysis, the length L_1 determining the in-band coupling strength can be used to meet the calculated coupling coefficient. Meanwhile, the second passband bandwidth will also be determined. Simulation and measurement were carried out using Zeland IE3D software and Agilent's 8719ES network analyzer. The

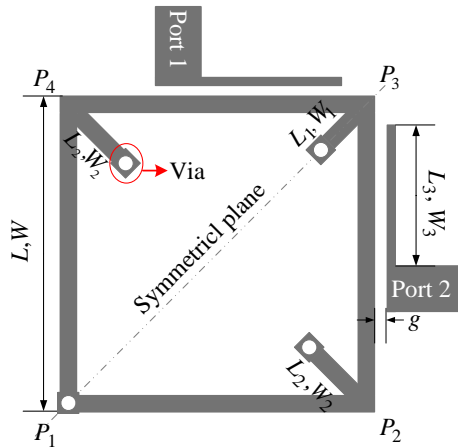


Figure 4. The configuration of dual-band BPF I. ($L = 32.1$ mm, $L_1 = 2.8$ mm, $L_2 = 8.1$ mm, $L_3 = 16$ mm, $W = W_1 = W_2 = 1$ mm, $W_3 = 0.2$ mm, $g = 0.2$ mm).

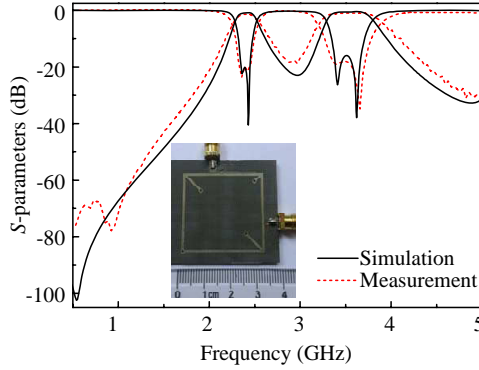


Figure 5. The simulated and measured results of the dual-band BPF I. (The inset shows a photograph of the fabricated filter).

final optimal geometric dimensions are listed in Figure 4. The designed filter was fabricated in microstrip technology, and the substrate with the relative dielectric constant of 2.45 and thickness of 1 mm was utilized.

Figure 5 shows the comparison of the simulated and measured results. There is some discrepancy between them due to unexpected tolerance in fabrication and implementation. The measured two passbands are centered at 2.4 and 3.5 GHz with 3 dB FBW of 9.2% and 17.1%. The measured insertion losses are 1.34 and 0.97 dB at the center frequencies. Meanwhile, good impedance matching can be seen, and the return losses are better than 18 dB in both passbands. Lastly, the circuit size of the fabricated filter is $0.37\lambda_g \times 0.37\lambda_g$ (λ_g is the guide wavelength of the first passband).

3.2. Dual-band BPF II with Source-load Coupling

As can be seen, the dual-band BPF I has a poor passband selectivity and band-to-band isolation. In order to solve this problem, a dual-band BPF II with source-load coupling was designed and fabricated as described in this section. Its configuration and final optimal geometrical dimensions are illustrated in Figure 6. For a compact size, the loop is meandered approximately without significant influence on resonant properties. Meanwhile, three short-stubs loaded at points P_2 , P_3 and P_4 are connected together by a common ground via-hole with a diameter of 1 mm. The gap g_2 between two feedline terminals is used to control the source-load coupling strength.

The simulated and measured results of the dual-band BPF II are

described in Figure 7(a), which shows a good agreement between them. The measured two passbands are centered at 2.4 and 3.5 GHz with 3 dB FBW of 17.1% and 7.9%. The measured insertion losses are 0.8 and 1.24 dB at the center frequencies. Meanwhile, the photograph of the fabricated filter is shown in Figure 7(b), and this has a much smaller circuit size $0.37\lambda_g \times 0.14\lambda_g$ in comparison with the dual-band BPF I. Due to the source-load coupling, both passbands exhibit high selectivity, and there are four transmission zeros located at 1.54, 2.97, 3.1 and 4.3 GHz. In addition, the band-to-band isolation level is better

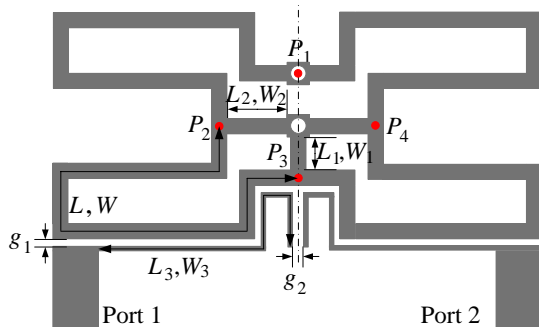


Figure 6. The configuration of dual-band BPF II. ($L = 32.1$ mm, $L_1 = 1.6$ mm, $L_2 = 4.9$ mm, $L_3 = 18.1$ mm, $W = W_1 = W_2 = 1$ mm, $W_3 = 0.2$ mm, $g_1 = 0.2$ mm, $g_2 = 1.2$ mm).

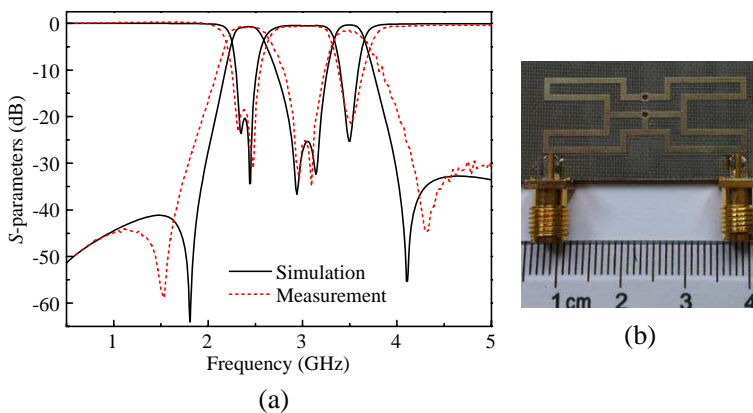


Figure 7. (a) The simulated and measured results of dual-band BPF II. (b) The photograph of the fabricated filter.

Table 1. Comparison of passband attenuation slop (AS) both filters. (AS_L and AS_R represent the attenuation slop of the left and right edge of a passband).

Filter	Band	Passband 1		Passband 2	
	AS	AS_L	AS_R	AS_L	AS_R
Filter I		54.56	42.83	56.39	28.87
Filter II		81.90	90.42	125.02	61.81

than that of the dual-band BPF I. Table 1 lists the comparison of the passband attenuation slopes of both filters. It can be observed that the dual-band BPF II has a sharper roll-off skirt selectivity than the dual-band BPF I.

4. CONCLUSION

In this paper, a novel square-loop quad-mode resonator is proposed and analyzed by even-odd-mode method. Through the analysis, both passband center frequencies can be controlled by the corresponding physical dimensions. Two filters based on the proposed resonator were designed, fabricated and measured, and good agreement was obtained between the simulated and measured results. Due to the introduction of source-load coupling in the dual-band BPF II, this exhibits better performance in passband selectivity and band-to-band isolation than the dual-band BPF I. The type of filter will be attractive in the wireless communication systems.

ACKNOWLEDGMENT

This work was supported by the National High Technology Research and Development Program of China (863 Program) No. 2012AA01A308 and the National Natural Science Foundation of China (NSFC) under Project No. 61271017 and 61072017.

REFERENCES

1. Ruiz-Cruz, J. A., M. M. Fahmi, and R. R. Mansour, "Triple-conductor combine resonators for dual-band filters with enhanced guard-band selectivity," *IEEE Trans. Microw. Theory Tech.*, Vol. 60, No. 12, 3969–3979, Dec. 2012.
2. Qin, W. and Q. Xue, "Complementary compact microstrip resonant cell and its applications to microwave single- and dual-band bandpass filters," *IEEE Trans. Microw. Theory Tech.*, Vol. 61, No. 2, 1829–1838, Feb. 2013.
3. Naglich, E. J., J. Lee, H. H. Sigmarsson, D. Peroulis, and W. J. Chappell, "Intersecting parallel-plate waveguide loaded cavities for dual-mode and dual-band filters," *IEEE Trans. Microw. Theory Tech.*, Vol. 61, No. 5, 1829–1838, May 2013.
4. Kuo, J.-T. and S.-W. Lai, "New dual-band bandpass filter with wide upper rejection band," *Progress In Electromagnetics Research*, Vol. 123, 371–384, 2012.
5. Kuo, J.-T., S.-C. Tang, and S.-H. Lin, "Quasi-elliptic function bandpass filter with upper stopband extension and high rejection level using cross-coupled stepped-impedance resonators," *Progress In Electromagnetics Research*, Vol. 114, 395–405, 2011.
6. Mondal, P. and M. K. Mandal, "Design of dual-band bandpass filters using stub-loaded open-loop resonators," *IEEE Trans. Microw. Theory Tech.*, Vol. 56, No. 1, 150–155, Jan. 2008.
7. Zhang, X. Y., J.-X. Chen, Q. Xue, and S.-M. Li, "Dual-band bandpass filters using stub-loaded resonators," *IEEE Microw. Wireless Compon. Lett.*, Vol. 17, No. 8, 583–585, Aug. 2007.
8. Wolff, I., "Microstrip bandpass filter using degenerate modes of a microstrip ring resonator," *Electron. Lett.*, Vol. 8, No. 12, 302–303, Jun. 1972.
9. Hong, J. S. and M. J. Lancaster, "Bandpass characteristics of new dual-mode microstrip square loop resonators," *Electron. Lett.*, Vol. 31, No. 11, 891–892, May 1995.
10. Hong, J. S. and H. Shaman, "Dual-mode microstrip open-loop resonators and filters," *IEEE Trans. Microw. Theory Tech.*, Vol. 55, No. 8, 1764–1770, Aug. 2007.
11. Athukorala, L. and D. Budimir, "Compact dual-mode open loop microstrip resonators and filters," *IEEE Microw. Wireless Compon. Lett.*, Vol. 19, No. 11, 698–700, Nov. 2009.
12. Sun, S.-J., B. Wu, T. Su, K. Deng, and C.-H. Liang, "Wideband dual-mode microstrip filter using short-ended resonators with centrally loaded inductive stub," *IEEE Trans. Microw. Theory*

- Tech.*, Vol. 60, No. 12, 3667–3673, Dec. 2012.
13. Sun, S.-J., S. Yang, B. Wu, K. Deng, and C.-H. Liang, “Dual-band bandpass filter using a single short-ended dual-mode resonator with adjustable first passband,” *Progress In Electromagnetics Research C*, Vol. 37, 95–106, 2013.
 14. Sun, S.-J., T. Su, K. Deng, B. Wu, and C.-H. Liang, “Shorted-ended stepped-impedance dual-resonance resonator and its application to bandpass filters,” *IEEE Trans. Microw. Theory Tech.*, Vol. 61, No. 9, 3209–3215, Sep. 2013.
 15. Luo, S. and L. Zhu, “A novel dual-mode dual-band bandpass filter based on a single ring resonator,” *IEEE Microw. Wireless Compon. Lett.*, Vol. 19, No. 8, 497–499, Aug. 2009.
 16. Sung, Y., “Dual-mode dual-band filter with band notch structures,” *IEEE Microw. Wireless Compon. Lett.*, Vol. 20, No. 2, 73–75, Feb. 2010.
 17. Li, Y. C., H. Wong, and Q. Xue, “Dual-mode dual-band bandpass filter based on a stub-loaded patch resonator,” *IEEE Microw. Wireless Compon. Lett.*, Vol. 21, No. 10, 525–527, Oct. 2011.
 18. Zhao, L.-P., X.-W. Dai, Z.-X. Chen, and C.-H. Liang, “Novel design of dual-mode dual-band bandpass filter with triangular resonators,” *Progress In Electromagnetics Research*, Vol. 77, 417–424, 2007.
 19. Chiou, Y.-C., P.-S. Yang, J.-T. Kuo, and C.-Y. Wu, “Transmission zero design graph for dual-mode dual-band filter with periodic stepped-impedance ring resonator,” *Progress In Electromagnetics Research*, Vol. 108, 23–36, 2010.
 20. Sun, S.-J., T. Su, K. Deng, B. Wu, and C.-H. Liang, “Compact microstrip dual-band bandpass filter using a novel stub-loaded quad-mode resonator,” *IEEE Microw. Wireless Compon. Lett.*, Vol. 23, No. 9, 465–467, Sep. 2013.
 21. Gao, L. and X. Y. Zhang, “High-selectivity dual-band bandpass filter using a quad-mode resonator with source-load coupling,” *IEEE Microw. Wireless Compon. Lett.*, Vol. 23, No. 9, 474–476, Sep. 2013.
 22. Cameron, R. J., “Advanced coupling matrix synthesis techniques for microwave filters,” *IEEE Trans. Microw. Theory Tech.*, Vol. 51, No. 1, 1–10, Jan. 2003.